LAWRENCE
LIVERMORE
NATIONAL
LABORATORY

LLNL-TR-403218

Modified Visible and Infrared Optical Design for the ITER Upper Ports

C.J. Lasnier, L.G. Seppala, K. Morris

April 25, 2008

Disclaimer

This work performed under the auspices of the U.S. Department of Energy by Lawrence Livermore National Laboratory under Contract DE-AC52-07NA27344.

Modified visible and infrared optical design for the ITER upper ports

C.J. Lasnier, L.G. Seppala, K. Morris

Lawrence Livermore National Laboratory

This work was performed under the auspices of the U.S. Department of Energy by Lawrence Livermore National Laboratory in part under Contract W-7405-Eng-48 and in part under Contract DE-AC52-07NA27344.
Work supported by the US ITER Project Office.

Abstract

This document reports the results of a follow-on optical design study of visible-light and infrared optics for the ITER[1] upper ports, performed by LLNL under contract for the US ITER Project Office. The major objectives of this work are to move the viewing aperture closer to the plasma so that the optical path does not cut through any adjacent blanket shield module other than the module designated for the port; move optics forward into the port tube to increase the aperture size and therefore improve the spatial resolution; assess the trade-off between spatial resolution and spatial coverage by reducing the field of view; and create a mechanical model with a neutron labyrinth.

Here we show an optical design incorporating all these aspects. The new design fits into a 360 mm ID tube, as did the previous design. The entrance aperture is increased from 10 mm to 21 mm, with a corresponding increase in spatial resolution. The Airy disk diameter for 3.8 μm wavelength IR light is 5.1 mm at the most distant target point in the field of view. The field of view is reduced from 60 toroidal degrees (full toroidal coverage with 6 cameras) to 50 toroidal degrees. The 10 degrees eliminated are those nearest the camera, which have the poorest view of the divertor plate and in fact saw little of the plate. The Cassegrain telescope that was outside the vacuum windows in the previous design is now in vacuum, along with lenses for visible light. The Cassegrain for visible light is eliminated. An additional set of optical relay lenses is added for the visible and for the IR.

[1] ITER.org January 2007, http://www.iter.org/

Executive summary

This report provides the results of an optical design study to revise the design of visible/IR camera optics for 6 upper ports of ITER, performed by Lawrence Livermore National Laboratory (LLNL) under contract to the US ITER Project Office. The previous design was also performed by LLNL for the USIPO under an initial scoping study[2], and the report of that work is available from the USIPO and from LLNL.

The changes to the optical design were planned to address the following issues. First, the viewing direction was corrected to be consistent with the fish-scale direction of the ITER divertor. Second, the entrance aperture of the optical system was moved toward the plasma along the optical axis into the blanket shield module, so that the optical path need not cut through an adjacent blanket shield module. Third, additional optics were introduced in the port plug to allow the use of a larger entrance aperture, which sets the diffraction-limited resolution of the system. Fourth, a mechanical model was created with a neutron labyrinth to facilitate later neutronics calculations.

The new optical design fits into a 360 mm ID tube, as did the previous design. The entrance aperture is now 21 mm compared to 10 mm in the old design, which improves the Airy disk diameter to 5.1 mm at the most distant target point in the view, for light of 3.8 μm wavelength. The detector pixel sizes of 20 μm for the IR and 10 μm for the visible detector are chosen to give a pixel spacing of 1.5 mm at the target, in keeping with the ITER specification 3 mm spatial resolution for the system.

The IR Cassegrain telescope that was outside the vacuum windows in the previous design is now inside the port tube, in vacuum. Also now in vacuum are lenses for the visible light. There is no Cassegrain now for the visible light. An additional stage of relay optics was added to the IR paths to compensate for the optics moved into the port plug.

The reason for this arrangement is that the materials used for IR lenses are more temperature-sensitive than the visible-light lenses. This motivated the use of the Cassegrain for IR in the port plug, where temperatures could routinely reach 200 C or more.

Performance requirements are given in the final report of the initial scoping study[2].

---

[2] C.J. Lasnier, L.G. Seppala, K. Morris, M. Groth, M.E. Fenstermacher, S.L. Allen, E. Synakowski, J. Ortiz, Visible and infrared optical design for the ITER upper ports, <http://www.pppl.gov/usiter-diagnostics/Instrumentation-Packages/Upper-IR-Visible-Cameras/ICP006779-A%20ITER%20Camera%20Report%20(LLNL).pdf>

I. Introduction

This report documents a revised optical design for visible/IR camera optics for the upper ports of ITER. The changes consist of correcting the viewing direction to the right instead of to the left, to be consistent with the fish-scale divertor design; moving the entrance aperture forward into the Blanket Shield Module so that the optical path does not cut through adjacent modules; reduction in the field of view from 60 toroidal degrees to 50 degrees in order to improve spatial resolution; and moving optics into the outer half of the port plug for the same purpose.

II. Optical design

The initial optical design used a 10 mm diameter aperture hole in the collector head. Although the IR optical performance was diffraction-limited, this hole size precluded imaging feature sizes smaller than about 8 mm in diameter at the 90 degree portion of the diverter ring. The study imposed several conditions that limited the hole in the collector head to 10 mm in diameter.

1. Each IR/visible camera imaged a 60 degree section (θ = 90 degrees to θ = 30 degrees) of the ITER torus in the region of the diverter ring. This annulus of about 1.5 m width was imaged with no vignetting.
2. The first IR and visible relay were about 4.0 m away from the collector head.
3. The visible and the IR optical relays were sized to fit inside of a 36 cm diameter tube. The aperture hole of the collector head was nearly in the center, 230 mm from the concave aspheric collector mirror.

The first IR and visible relays were both Cassegrain-type telescopes, 20 and 10 cm in diameter, with aspheric corrector plates The IR and visible beam were separated at this point where the optical collector head imaged the aperture hole. There was an additional refractive relay for both the IR and visible that put camera images about 10 m from the collector head just past the outer bioshield wall.

Current design study:

Several conditions have been relaxed to allow the aperture hole in the collector head to grow from 10 mm to 21 mm in diameter, while still maintaining a 36 cm diameter tube.

1. Reduced field coverage: Each IR/visible camera now images only a 50 degree section (θ = 90 degrees to θ = 40 degrees) of the ITER torus in the region of the diverter ring. The field is vignetted so that only the portion of the annulus near the diverter ring

at θ = 90 degrees and at θ = 40 degrees is imaged. Some portions of the full 1.5 m annulus at these limiting angles cannot be seen.

2. The first IR and visible relay have been moved to about 2.0 m from the collector head, 50% closer than the original 4.0 m distance.
3. The aperture hole is moved as far away as possible from the aspheric collector mirror, 306 mm from the concave aspheric collector mirror.

Most of the tube diameter is devoted to the IR channel The IR optical relays occupy a maximum diameter of 21 cm and the visible relay use up the remaining 15 cm of the 36 cm inner diameter of the transport tube. This choice has led to a design in which the visible has 2x better resolution even though nearly 80% of the collected energy is directed to the IR channel.

With the larger hole size, the IR imaging capability (still diffraction-limited) is extended so that feature sizes around 3 to 4 mm in diameter at the 90 degree portion of the diverter ring can be seen. At the same time, the last IR and visible optical relays are now sufficiently beyond the outer bioshield wall so that a fold mirror can be inserted between the wall and the final optical relay. The detectors, located about 12 m from the collector head, can be better protected in this geometry. Because the IR camera now collects an etendue (product of solid angle collected and optical area of the relay optics) over 4 times larger than the previous design, the optical relays between the collector head and the camera are more complex. There are now two IR refractive relays instead of one beyond the IR Cassegrain relay. The visible relaying has been simplified by replacing the Cassegrain telescope with a refractive relay. A single refractive relay stage, after a fold mirror beyond the bioshield wall, relays an image to the CCD detector.

The IR relays use three materials: zinc selenide, zinc sulfide and germanium. The optical design has five or six lenses per relay telescope.

Near-diffraction-limited performance across the broad spectrum of 400 nm to 700 nm requires apochromatic correction in which three wavelengths are brought to a common focus. Normal achromatic correction, in which two wavelength are brought to a common focus, can be achieved with two glass types, but the resolution is far from diffraction-limited. In this severe radiation environment, the choice for a two-glass achromatic solution is synthetic fused silica and calcium fluoride. Performance is less than ideal with a Strehl ratio of around 15%. The best focal spot that can be achieved corresponds to a diameter of about 5 mm in ITER at the 90 degree position. An apochromatic solution was obtained by adding a third glass type. Several choices are possible, but Schott radiation resistant glass LF5G15, with index 1.584 at 589 nm and Abbe dispersion 40.8 gives good transmission in the UV. The transmission of a 10 mm

substrate is 86% at 420 nm and 60% at 400 nm. Using this three-glass combination, the Strehl ratio is greater that 90% across the full field and the corresponding spot size at the 90 degree positioning in the ITER chamber is about 2.0 mm.

The aperture hole area is shared by both the IR and visible channels. About 79% of the area is used to collect the IR and about 13%is devoted to the visible. The IR and visible beams overlap in about 8% of the area and is excluded from being collected.

Effects of reducing the field coverage

Figure 1 shows both the original field of the IR/visible diagnostic (larger circle) and the current field of view (smaller circle).

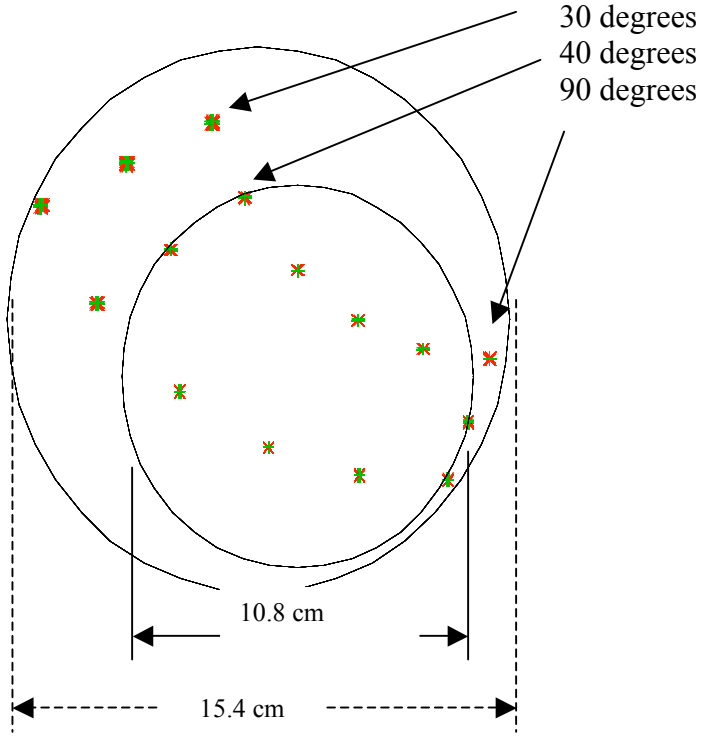

Figure 1. Reduced field at image plane of collector.

The etendue or total collection of light is proportional to the product of the object area and the area of the aperture hole. For a given etendue, a reduction in object area and diameter means that diameter and area can be increased.

Figure 1 show the effects of reducing the field coverage. The red dots show the images collected by the current aspheric mirror in the collector head, located 306 mm from the 21 mm aperture hole. The image diameter for full collection of the 60 degree annular ring is 15.4 cm in diameter. By reducing the field coverage to 50 instead of 60 degrees and requiring only the center ring to be imaged at the ends, the image diameter can be reduced to 10.8 cm, 30% smaller in diameter and 50% smaller in area.

Optical imaging performance at the 90 degree position

The limiting optical resolution is set by diffraction since both the IR and visible channels are diffraction-limited. The distance from a point on the diverter ring at the 90 degree position to the collector head is 11.5 m. While the IR channel uses the entire 21 mm hole, only a 7.4 mm diameter hole is used for the visible. The Airy diameter is :

Airy diameter = $2.44 \lambda z / d$ where λ= wavelength of light, z = distance to collector head and d = the effective aperture hole diameter. The results are shown in Table 1.

Table 1. Airy disk diameter

Wavelength (microns)	Aperture diameter (mm)	Distance to collector head (mm)	Airy disc diameter (mm)
0.00380	21.0	11500	5.1
0.00055	7.4	11500	2.1

The corresponding diffracted spot sizes for a 21 mm diameter hole (IR) and a 7.4 mm effective hole (visible) are shown below in Figure 2 and Figure 3, respectively.

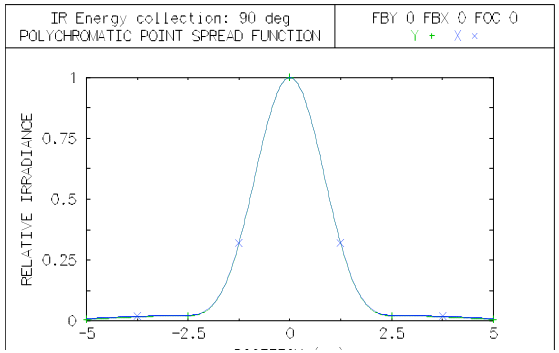

Figure 2. The Airy disc, for a point on the camera projected back to the 90 degree position of the diverter ring, is 5.1 mm in diameter.

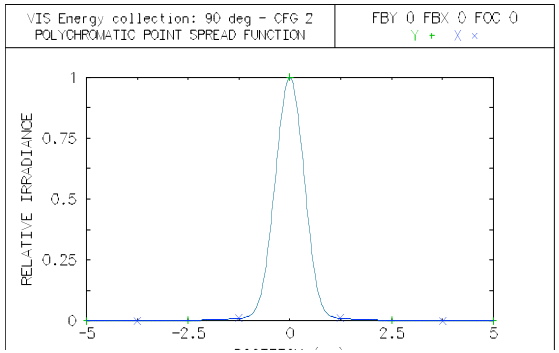

Figure 3. The Airy disc, for a point on the camera projected back to the 90 degree position of the divertor ring, is 2.1 mm in diameter.

The energy collected within a given diameter circle is shown in Figure 4 (IR) and Figure 5 (visible). The modulation transfer functions for the IR and visible are shown in Figure 6 and Figure 7, respectively.

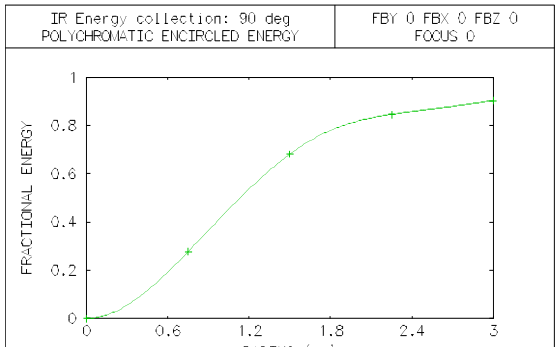

Figure 4. IR resolution: About 50% of the energy is collected within a 3 mm diameter circle diameter at the 90 degree position of the divertor ring.

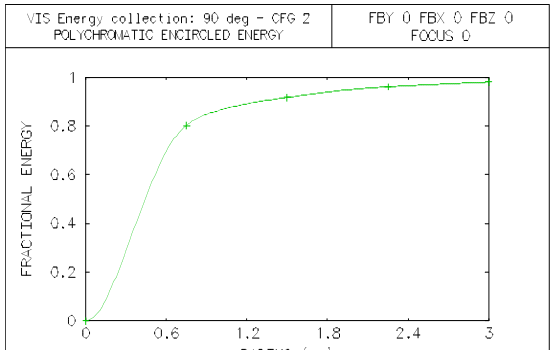

Figure 5. Visible resolution: About 90% of the energy is collected within a 3 mm diameter circle at the 90 degree position of the divertor ring.

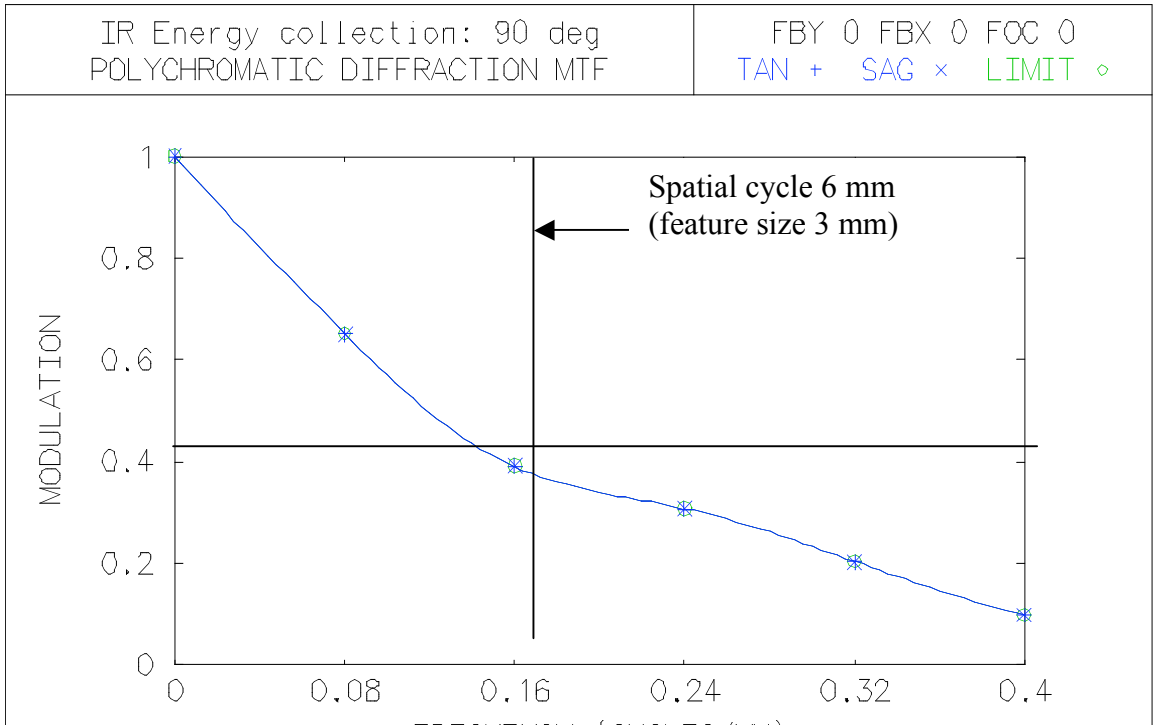

Figure 6. IR contrast: The contrast for an object with a 6 mm period (3 mm features) is about 40% at the 90 degree position of the diverter ring.

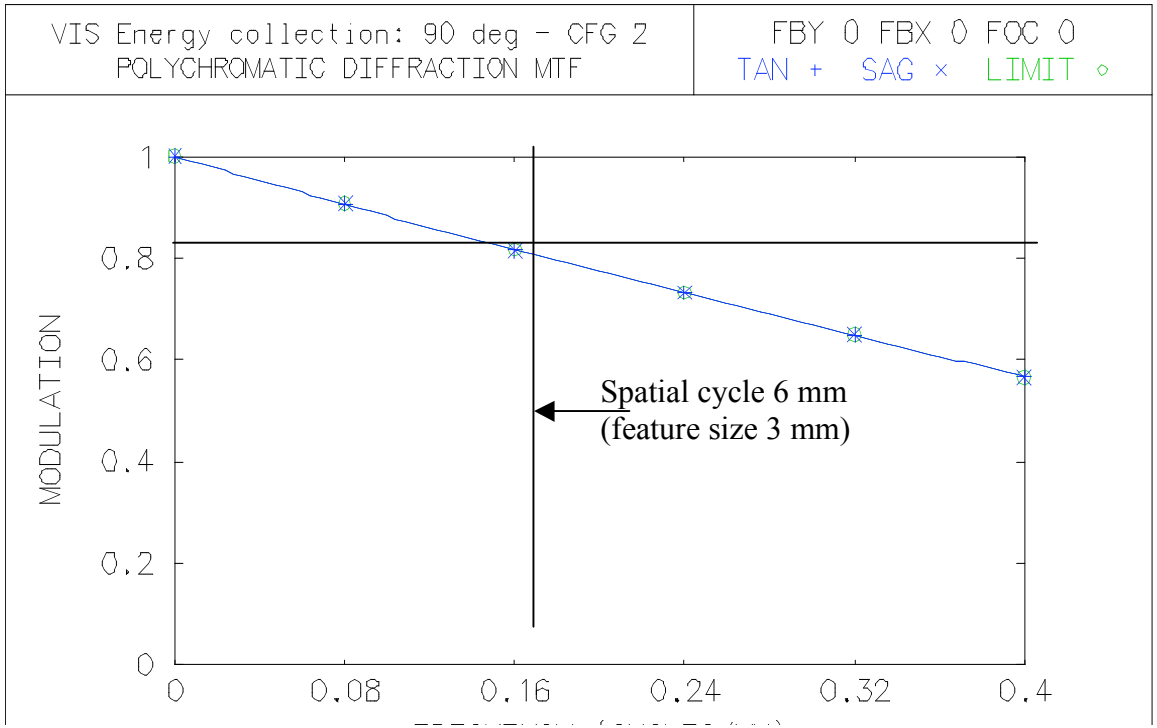

Figure 7. Visible contrast: The contrast for an object with a 6 mm period (3 mm features) is about 80% at the 90 degree position of the diverter ring.

Camera size for IR and visible imaging:

The camera has been sized so that each pixel, projected back to the 90 degree position on the diverter ring, subtends a 1.5 mm width. At angles less than 90 degrees, the projected pixel width is smaller. The detector size data is given in Table 2.

Table 2. Camera detector size.

	Camera width (mm)	Diverter to camera magnification^{-1}		Pixel size (mm)	Pixel size projected to diverter ring (mm)		Camera width in pixels
		θ=90 deg	θ=50 deg		θ=90 deg	θ=50 deg	
IR	70	75	55	0.02	1.5	1.1	3500
Visible	35	150	110	0.01	1.5	1.1	3500

At the IR camera and visible camera, respectively, the focal ratios are about f/9 and f/12. The focal ratio varies by +/- 15% depending on the position on the diverter ring.

The optical prescription for the IR components is given in Table 3. The aspheric coefficients are given in Table 4 for the surfaces referenced in Table 3. The comparable prescription for the visible components is given in Table 5 and Table 6.

Table 3. Optical prescription for the IR beam components.

Surface #	Radius of curvature (mm)	Thickness (mm)	Semi-aperture diameter (mm)	Material	Note
Object	--	7495	6417	AIR	
Aperture	--	306.00	10.50	AIR	
2	-554.306	-306.00	76.00	Mirror	Aspheric mirror
3	--	1068.92	78.00	Mirror	Collector fold
4	--	-180.00	104.00	Mirror	M3 fold
5	--	845.00	110.00	Mirror	M4 fold
6	--	50.00	100.00	AIR	
7	521000.000	12.50	95.00	ZNSE	T1C1 aspheric
8	--	12.50	100.00	AIR	
9	--	458.10	100.00	AIR	
10	-1011.000	-458.10	105.00	Mirror	T1M1
11	-522.000	459.10	37.00	Mirror	T1M2
12	--	1.00	40.00	AIR	
13	--	35.00	35.50	AIR	Image relay
14	--	7.00	47.00	SAPPHIRE	Vacuum window
15	--	15.00	47.00	AIR	
16	--	7.00	47.00	SAPPHIRE	Vacuum window
17	--	10.00	47.00	AIR	
18	-909.000	9.00	50.00	ZNS	F1L1
19	-938.800	255.20	50.00	AIR	
20	-3855.000	15.40	80.00	ZNSE	F1L2
21	-782.000	1617.00	80.00	AIR	
22	407.500	20.00	80.00	ZNSE	R1L1
23	1615.700	53.00	80.00	AIR	
24	407.500	20.00	70.00	ZNSE	R1L2
25	1615.700	0.79	70.00	AIR	
26	1125.800	15.00	70.00	GERM	R1L3

27		665.300	5.60	70.00	AIR	
28	--		13.00	70.00	ZNS	R1L4
29		240.300	326.70	70.00	AIR	
30	--		15.00	70.00	GERM	R1L5
31		-11298.000	7.80	70.00	AIR	
32		-390.400	15.00	70.00	ZNS	R1L6
33		-314.700	2878.40	70.00	AIR	
34	--		15.00	92.00	ZNSE	F2 f
35		-2263.000	725.00	65.00	AIR	
36	--		2037.00	100.00	AIR	Bio-inner
37	--		195.00	100.00	AIR	Bio-outer
38	--		-125.00	125.00	Mirror	Fold mirror
39		-640.300	-20.00	91.00	ZNSE	R2L1
40	--		-65.00	91.00	AIR	
41		-640.300	-20.00	75.00	ZNSE	R2L2
42	--		-3.16	75.00	AIR	
43		933.000	-15.00	75.00	GERM	R2L3
44		1392.000	-2.50	75.00	AIR	
45		802.000	-13.00	75.00	ZNS	R2L4
46		-491.000	-93.20	75.00	AIR	
47		270.000	-14.00	73.00	ZNS	R2L5
48		216.000	-65.00	76.00	AIR	
49	--		-1016.60	128.41	AIR	Cold stop
Image	--		--	35.00		Camera plane

Table 4. Aspheric coefficients for the IR optics. Reference the surface number in Table 3.

Aspheric coefficients

SRF	CC	AD	AE	COMPONENT
2	-0.658	0.0	0.0	COLLECTOR MIRROR

7	0.000	-1.071E-10	0.0	CASSEGRAIN CORRECTOR
11	0.000	1.274E-09	0.0	SECONDARY MIRROR

Table 5. Optical prescription for the visible beam components.

Surface number	Radius of curvature (mm)	Thickness (mm)	Semi-aperture diameter (mm)	Material	Note
Object	--	7495	6417	AIR	
1	--	306.00	10.5	AIR	
2	-554.306	-306.00	68	Mirror	Aspheric mirror
3	--	1068.92	68	Mirror	Collector fold
4	--	-180.00	104	Mirror	M3 fold
5	--	795.00	110	Mirror	M4 fold
Aperture	--	50.00	25	AIR	
7	--	-180.00	50	Mirror	M5 fold
8	--	295.00	58	Mirror	M6 fold
9	--	7.00	58	SILICA	R1L1
10	250.000	0.25	58	AIR	
11	250.000	17.00	58	CAF2	R1L2
12	-538.550	254.20	58	AIR	
13	--	12.00	47	SILICA	Vacuum window
14	--	5.00	58	AIR	
15	--	12.00	47	SILICA	Vacuum window
16	--	2795.00	58	AIR	
17	--	10.00	279.53118	SILICA	Field lens

18		-1077.500	3207.55	70	AIR	
19	--		2037.00	69	AIR	Bio-inner
20	--		135.00	69	AIR	Bio-outer
21	--		-100.00	100	Mirror	
22		-478.600	-12.00	70	SILICA	R2L1
23		-224.000	-3.35	70	AIR	
24		-226.350	-25.00	70	CAF2	R2L2
25	--		-780.70	70	AIR	
26		327.600	-6.00	42	LF5G15	R2L3
27		-9638.000	-0.10	42	AIR	
28		-689.800	-10.00	42	SILICA	R2L4
29		689.800	-533.10	42	AIR	
30		-1178.600	-10.00	42	LF5G15	R2L5
31		1178.600	-381.40	42	AIR	
Image	--		--	18		Camera

Table 6. Aspheric coefficients for the first mirror (same as for IR) (Reference the surface number in Table 5).

Aspheric coefficients			
SRF	CC	AD	AE
2	-0.658	0.0	0.00

Testing and alignment of IR optical relays:

Optical collector head

A common reflective optical relay in the collector head (Figure 8) is used to image a 50 degree wide annulus around the diverter ring. The first optical element is a concave mirror that is a conic section, located 306 mm from the aperture hole. Two parameters fully describe the conic section. The radius of curvature (R = 534.3 mm) is chosen to image a 21 mm diameter aperture hole onto the 200 mm diameter primary mirror of the Cassegrain, located 2.0 m from the collector head. The conic constant (k= -0.656) is chosen to provide the best imaging between the 21 mm hole and the primary mirror.

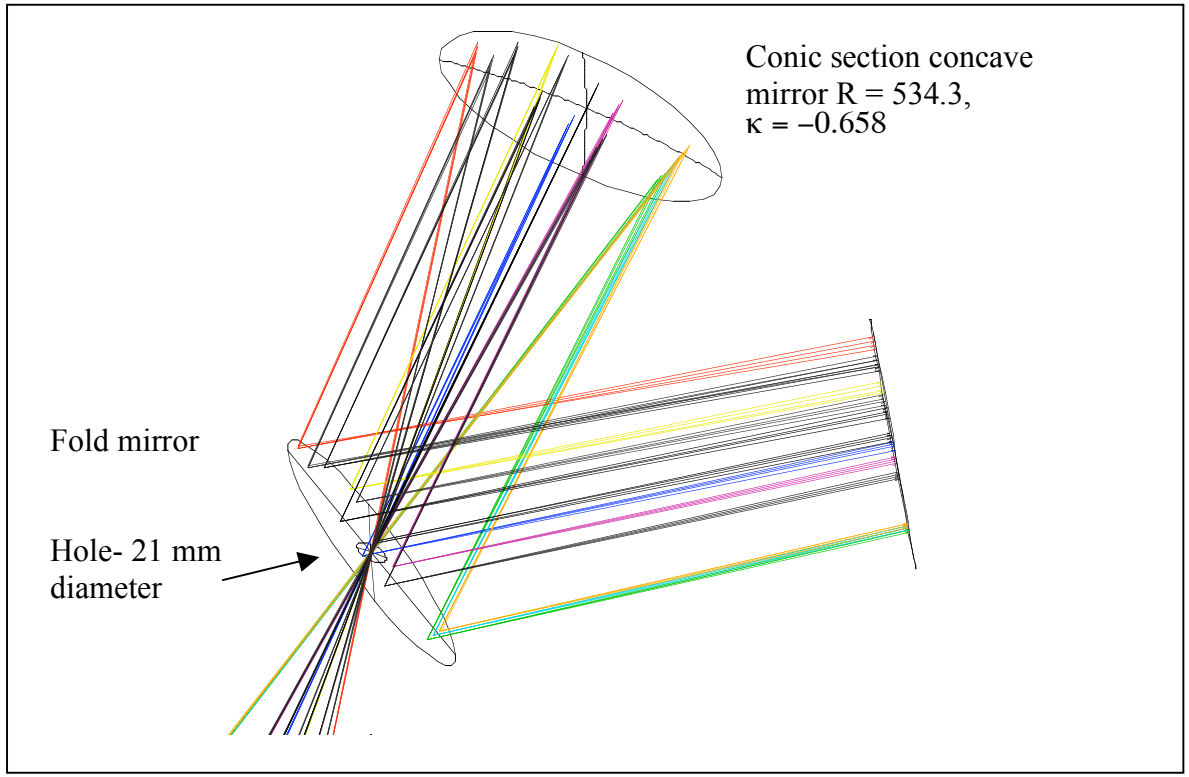

Figure 8. Optical collector head

There are no remaining degrees of freedom to optimize the optical imaging performance. Fortunately, the images formed by this mirror across the annular 50 degree ring are diffraction-limited. Figure 9 shows the geometrical spot sizes across the compared to the Airy disc diameter.

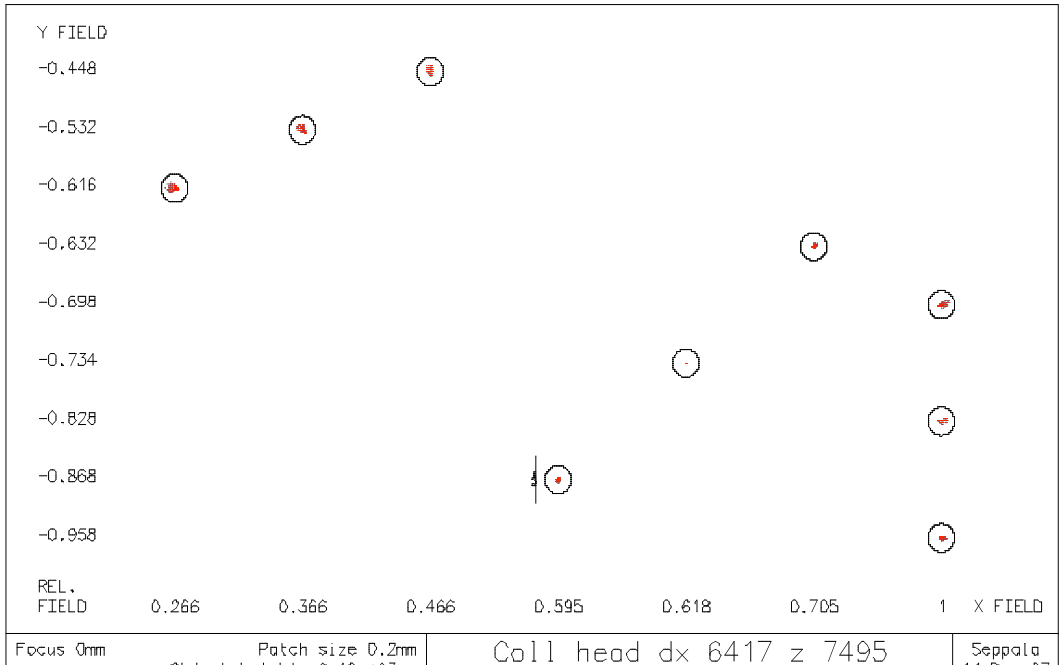

Figure 9. Geometrical spot sizes formed by the aspheric collector mirror are small compared to the diameter of the Airy disc.

Design method for optical relays, IR and visible

The IR and visible beam lines contain multiple image relaying telescopes. The end-to-end IR and visible systems are required to be diffraction-limited so that the maximum resolution can be achieved, given a particular aperture hole size and ITER geometry. Assembly and alignment becomes problematic if each individual relay cannot easily be tested. Each individual relay should be capable of being fabricated, aligned and tested by itself. The full assembly of the entire beam line is much less sensitive to alignment errors, since one relay is not compensating for aberrations caused by another relay.

The actual optimization is accomplished in the OSLO optical design program. OSLO allows a simple method for designing multiple configurations. In the case of the IR system, four configurations are simultaneously optimized:

1. End-to-end Cassegrain telescope, two refractive relay telescopes and the required field lenses. The final camera image plane is tilted by about 1 degree to compensate for the nearly 30 degree tilt of the object plane.
2. Stand-alone Cassegrain telescope.
3. First refractive relay telescope.
4. Second refractive relay telescope

In the case of the visible system, three configurations are simultaneously optimized:

1. End-to-end refractive telescopes and a field lens. The final camera image plane is tilted by about 1 degree to compensate for the nearly 30 degree tilt of the object plane.
2. First refractive relay telescope.
3. Second refractive relay telescope.

The following five figures (Figures 10-14) show configurations for testing each of the three IR relay telescopes and the two visible relay telescopes. Each telescope will in general have a curved focal plane since the total system has flat object and image planes.

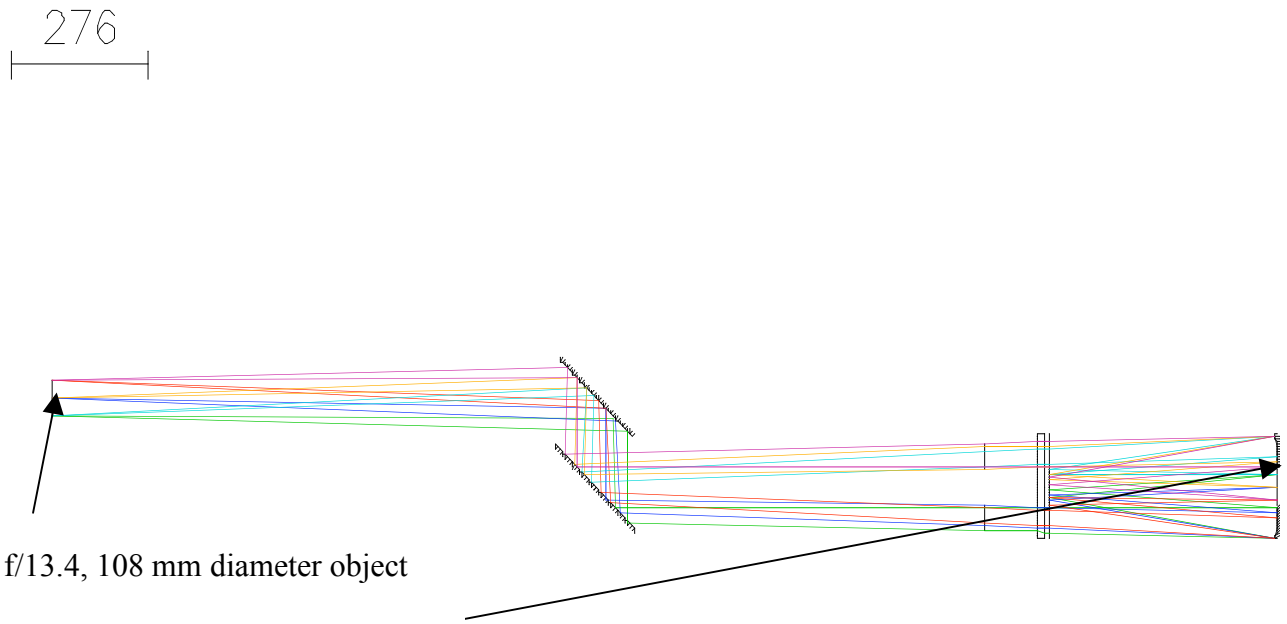

Figure 10. IR Cassegrain telescope assembly test

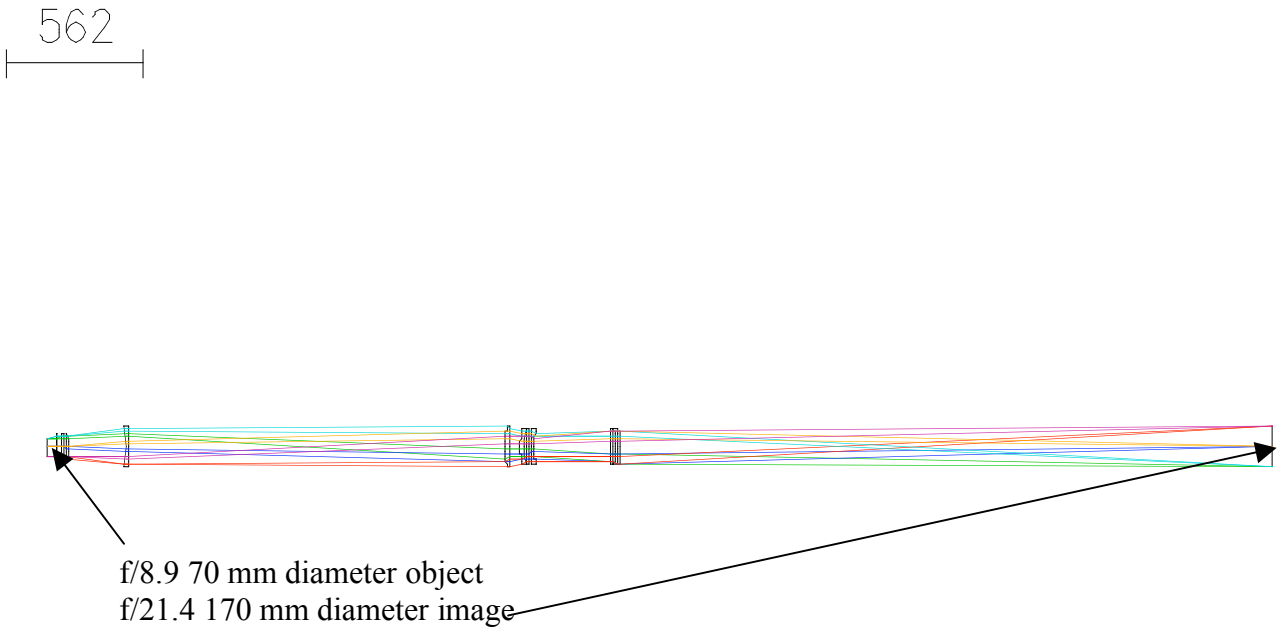

Figure 11. IR first refractive relay.

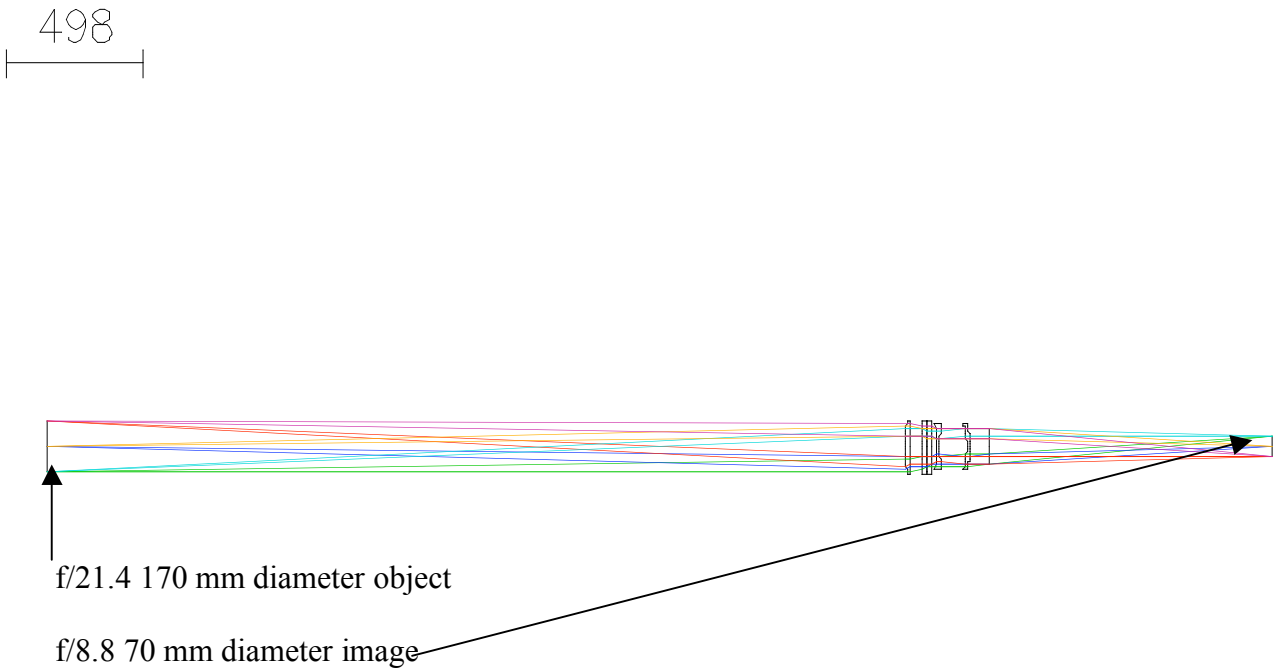

Figure 12. IR second refractive relay.

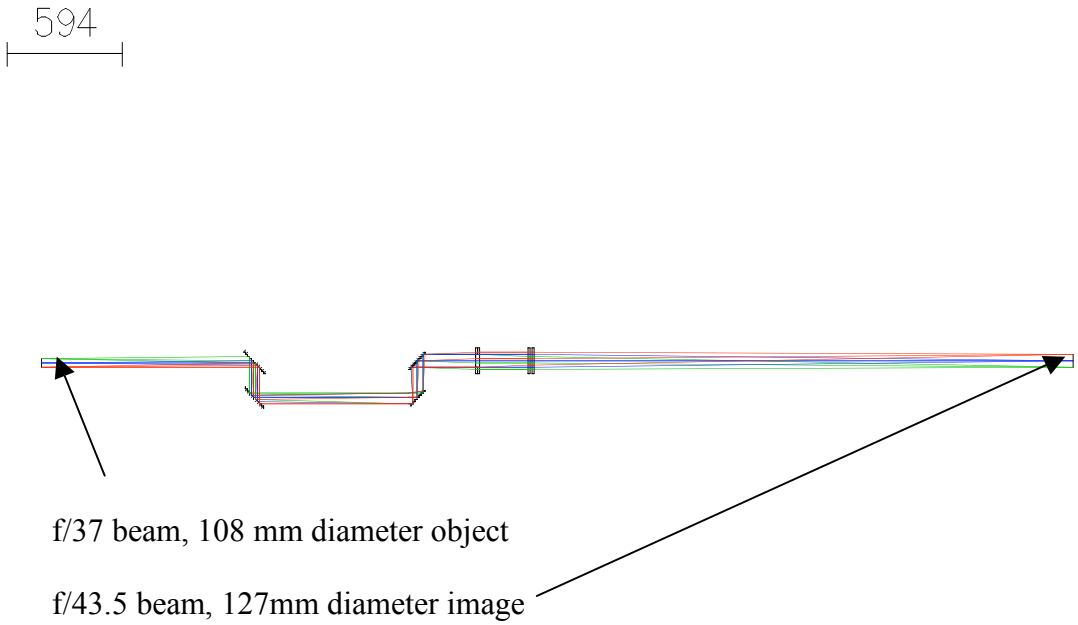

Figure 13. Visible first refractive relay.

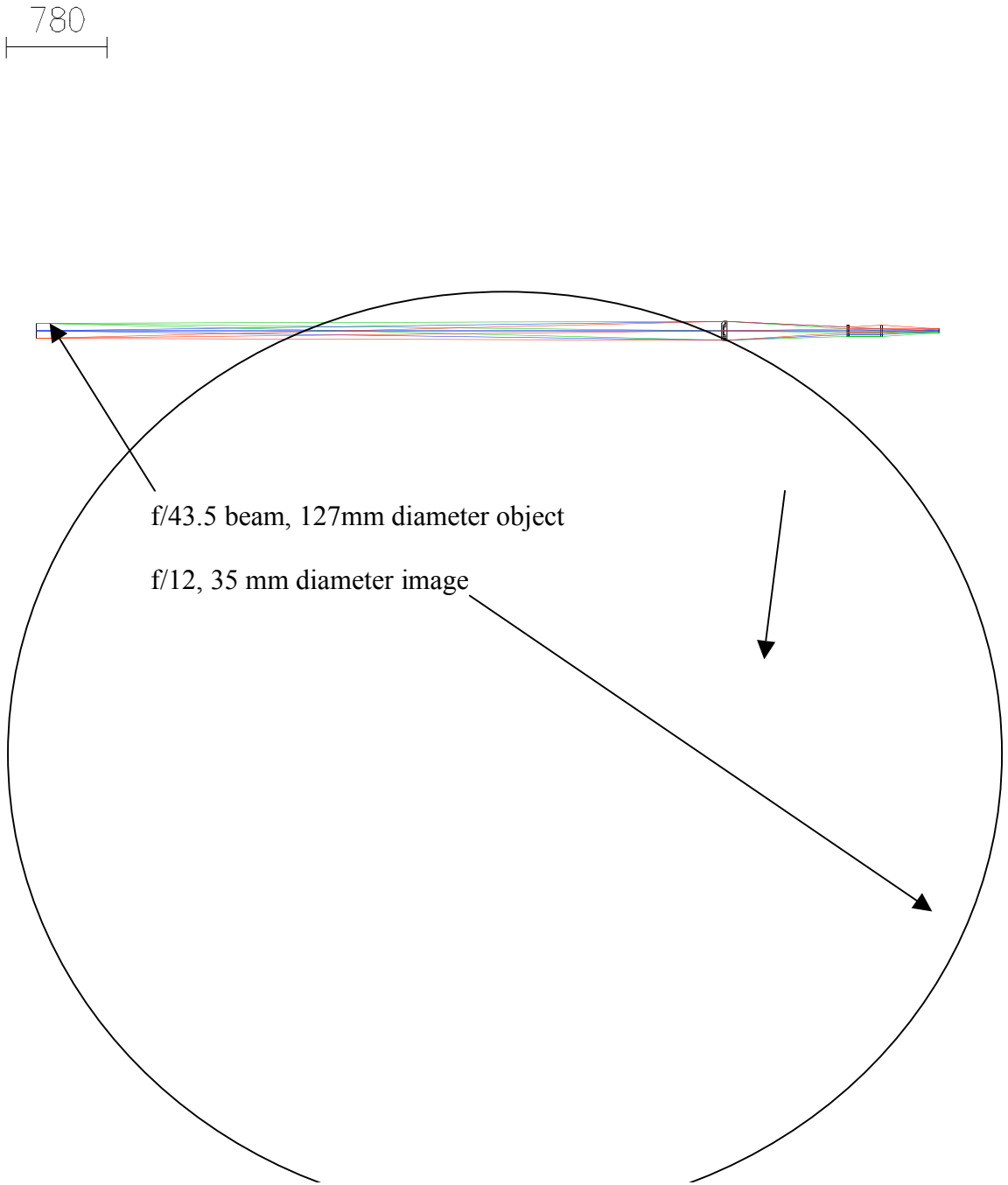
780
f/43.5 beam, 127mm diameter object
f/12, 35 mm diameter image

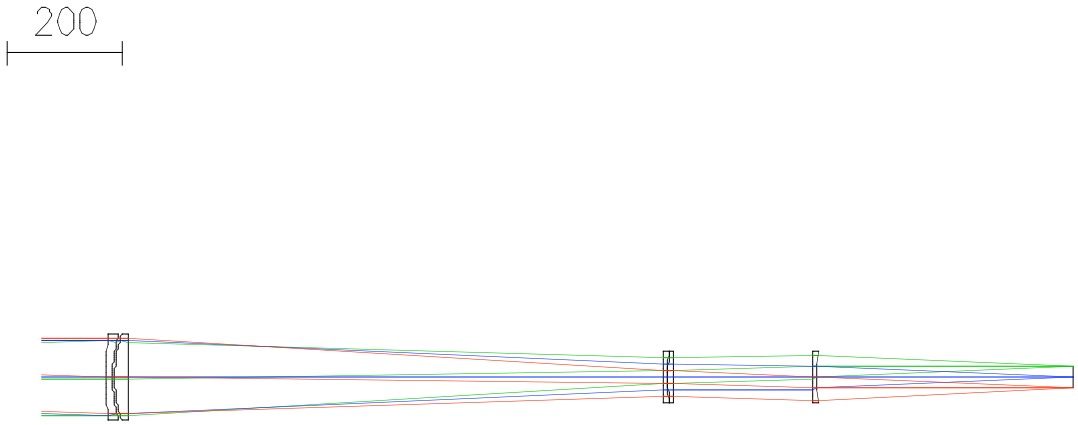
200

Figures 15-18 show optical layouts and features for the IR and visible channels inside a 36 cm diameter tube.

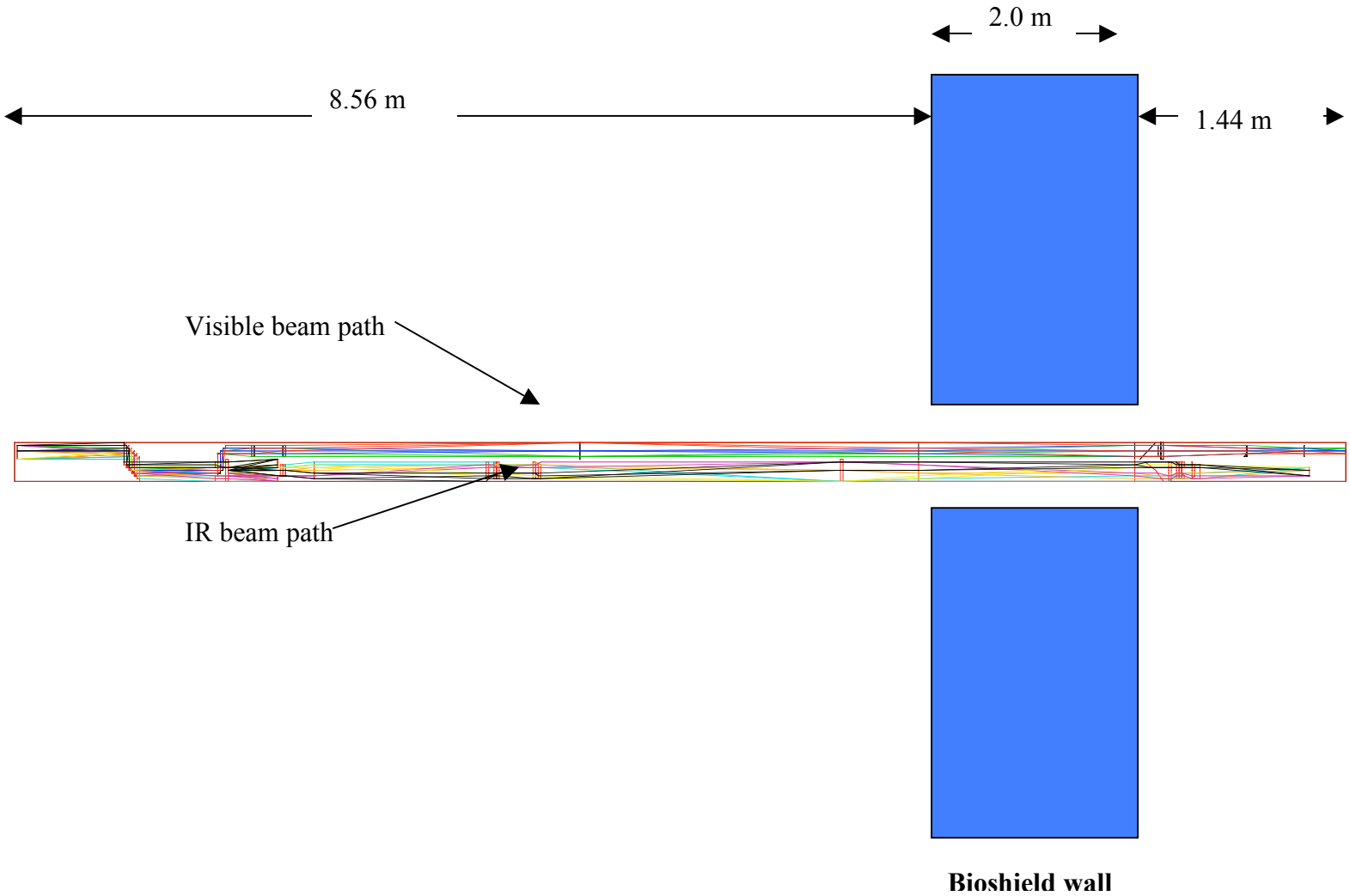

Figure 15. The 36 cm diameter tube contains both the IR and visible optical relays to the IR and visible cameras.

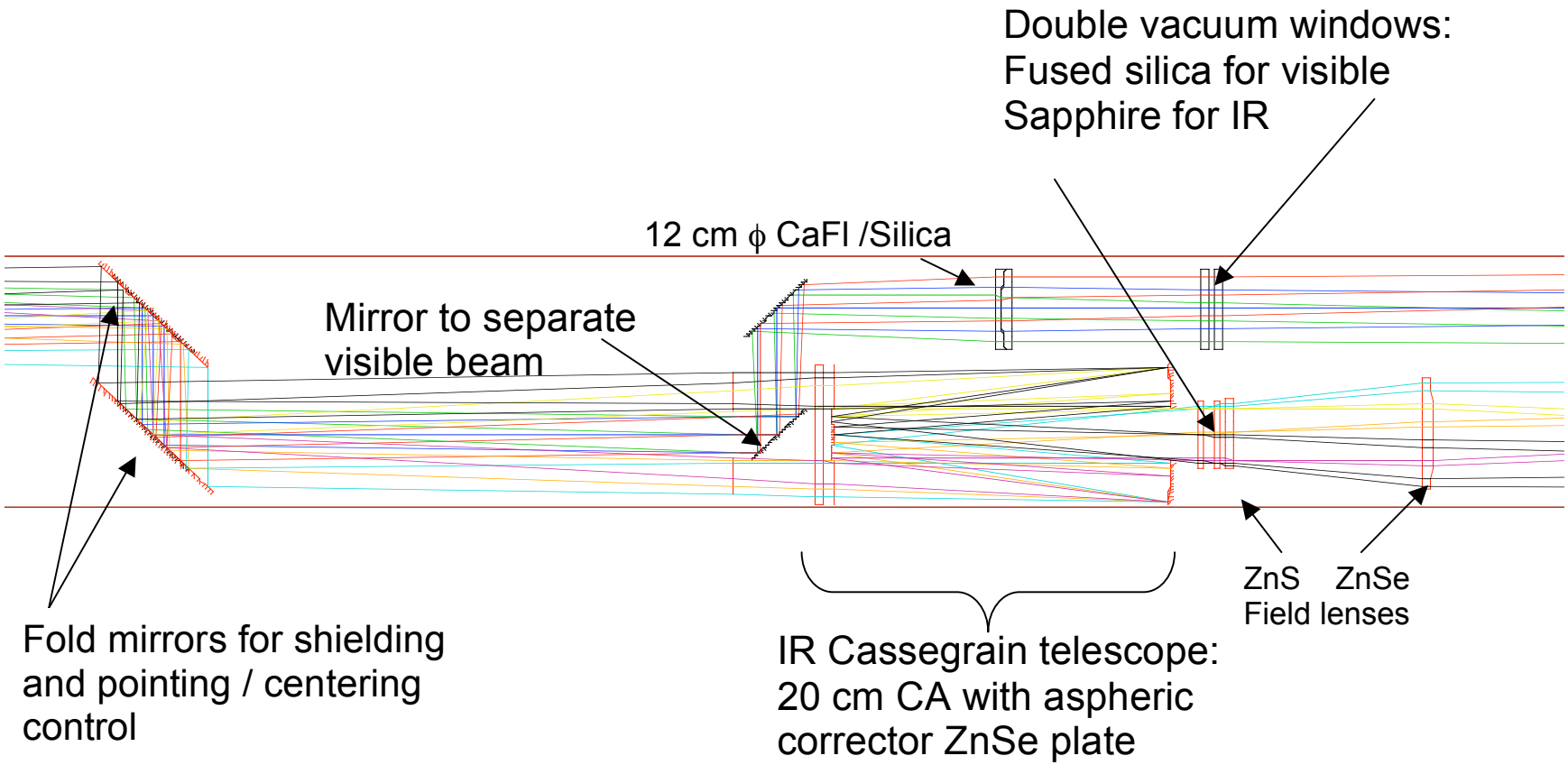

Figure 16. Details of first relays after splitting of IR and visible beams. The limiting aperture for the IR beam is the primary mirror of the Cassegrain telescope. The central obscuration of the telescope is 46% of the 20 cm diameter. The aperture hole should be sufficiently large to allow for imperfect imaging between this hole and the primary mirror and for small misalignments of the mirrors. The limiting aperture for visible beam is the small 45 degree mirror that separates the IR and visible beams. Necessarily, this aperture cannot be exactly imaged onto the aperture hole. However, since the visible beam uses 35% of the full beam, the defocused beam is still well within the 21 mm hole. While the beam at the separation mirror is only 5 cm in diameter, the first visible relay must be about 12 cm in diameter so that all object beams can pass without vignetting.

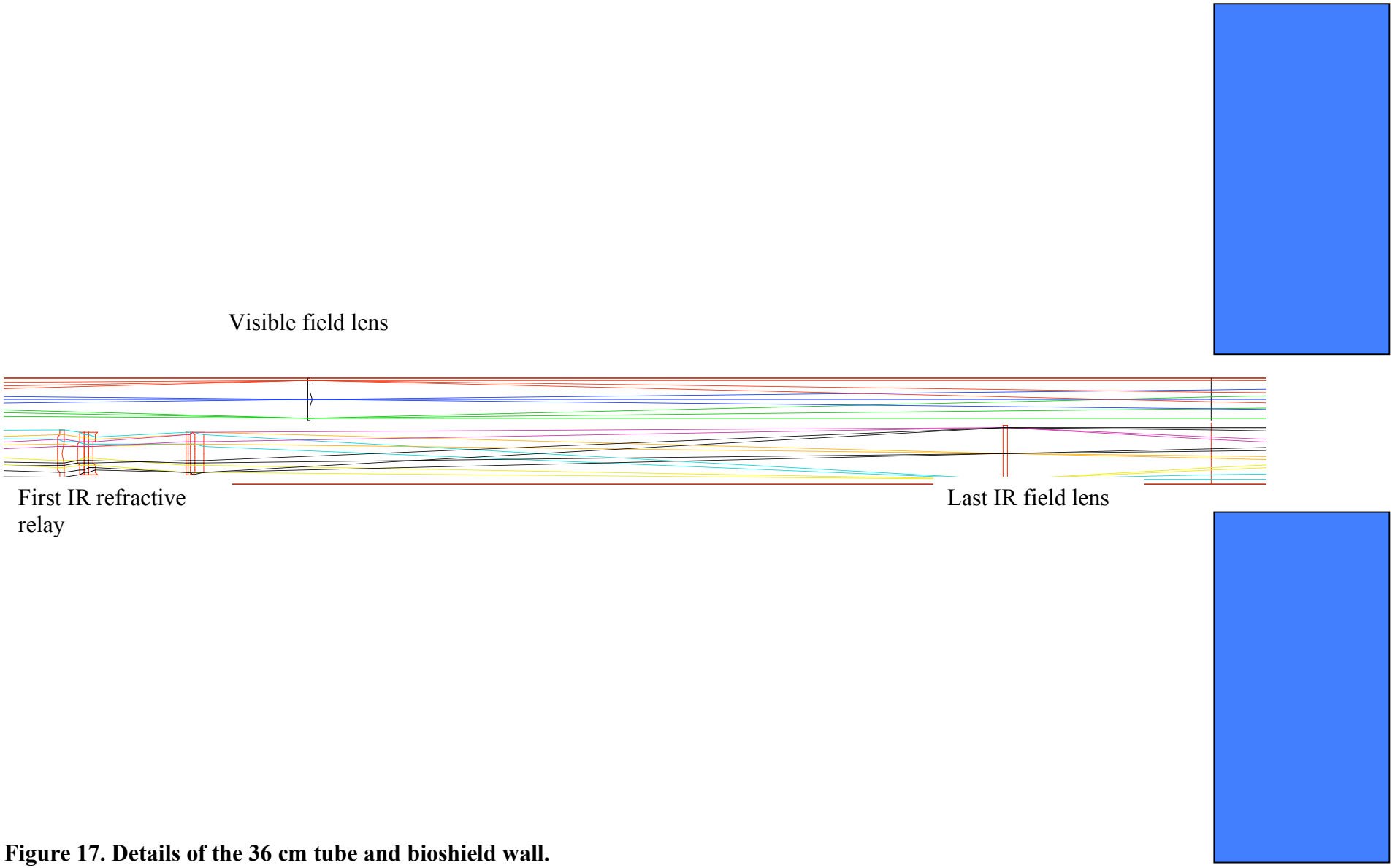

Figure 17. Details of the 36 cm tube and bioshield wall.

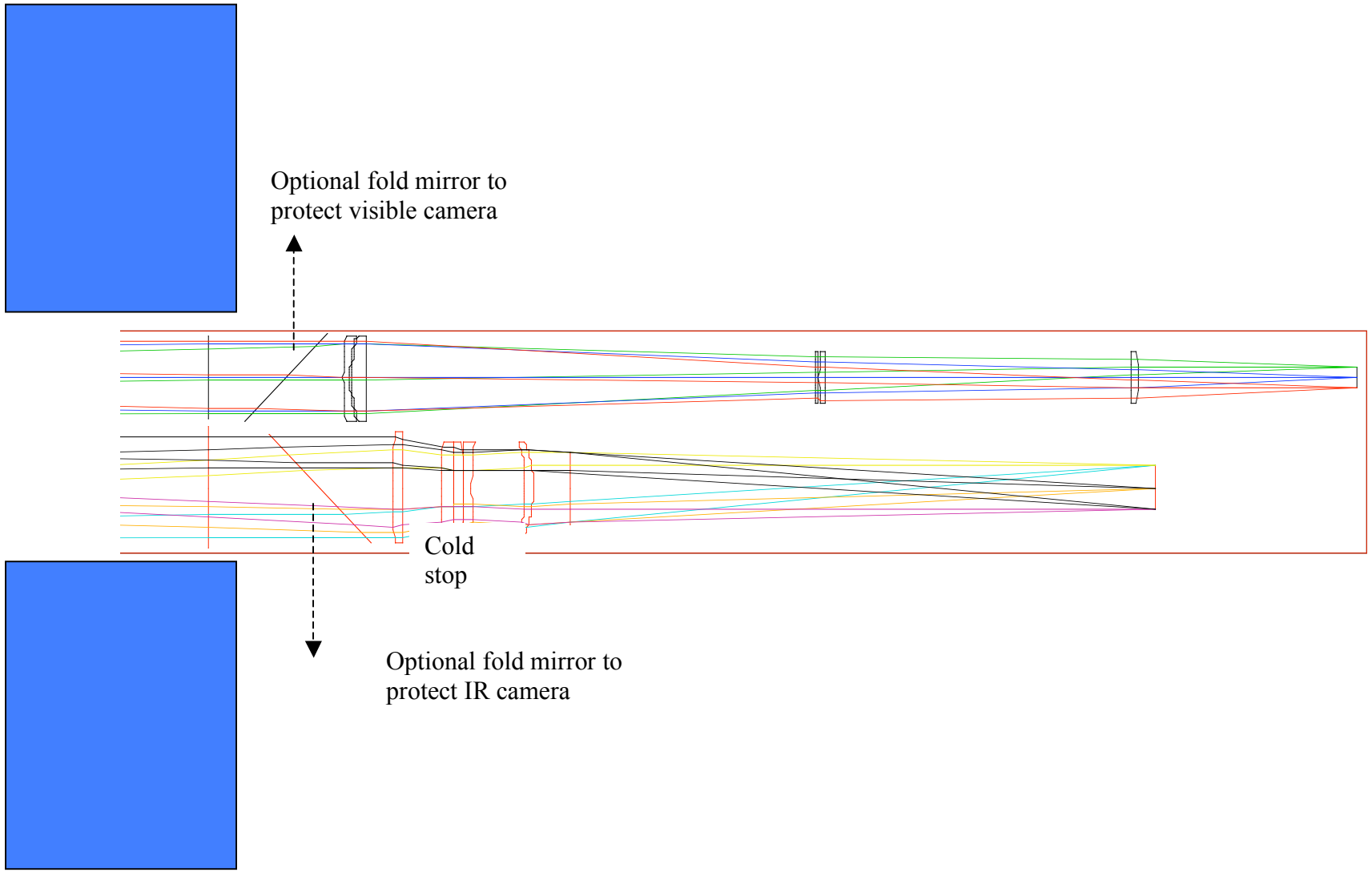

Figure 18. Details of the 36 cm diameter tube after the bioshield wall.

III. Drawings of the system

This section contains drawings of the system in place in the port plug, starting with overviews, then closer views starting at the inner (plasma) end and moving outward through the port plug, port interspace, and bioshield wall.

Figure 19 shows an overview of the system including the port, the cameras, and the field of view at the divertor of one system. The blue tube passes through the port interspace. Figure 20 shows a cutaway view of the optical tube and port plug. Figure 21 shows a closer view of the port plug and optical tube.

Figure 22 shows the area of the divertor viewed by one system. Figure 23 shows this from another angle. Figure 24 shows more clearly how the viewing area is displaced toroidally from the camera location. Figure 25 shows the path of light entering through an opening in the Blanket Shield Module. Figure 26 shows a close view of the first optical head, consisting of the first two mirrors. The location of the aperture in the blanket shield module is also seen.

Figure 27 shows a side view of optics in the port plug. The blue shaded areas represent neutron shielding material, with penetrations for the beam path. The IR Cassegrain telescope is shown, as well as the pickoff mirror for the visible light view. Figure 28 shows a closer view of the Cassegrain and vacuum windows. Each of the visible and IR paths has the required double vacuum window. The IR path has an additional corrector plate near the windows. Figure 29 shows the vacuum windows and an IR relay optics set.

Figure 30 shows the IR relay optics near the end of the port plug. The IR beam is on top and the visible beam is below it. In Figure 31 we see relay optics in the portion of the optical tube outside the bioshield, and turning mirrors for the IR and visible beams. The turning mirrors allow us to move the cameras out of the direct path to reduce neutron exposure. Figure 32 shows the entire end section including the cameras.

Figure 33 depicts the optical tube passing through the bioshield.

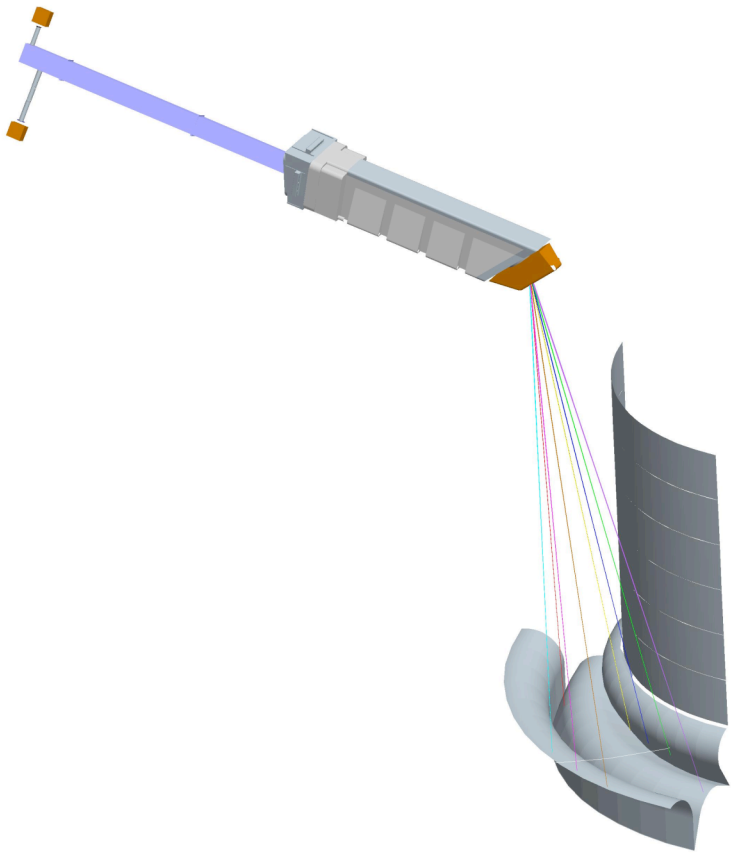

Figure 19. Overview of the system, showing the optical path and divertor.

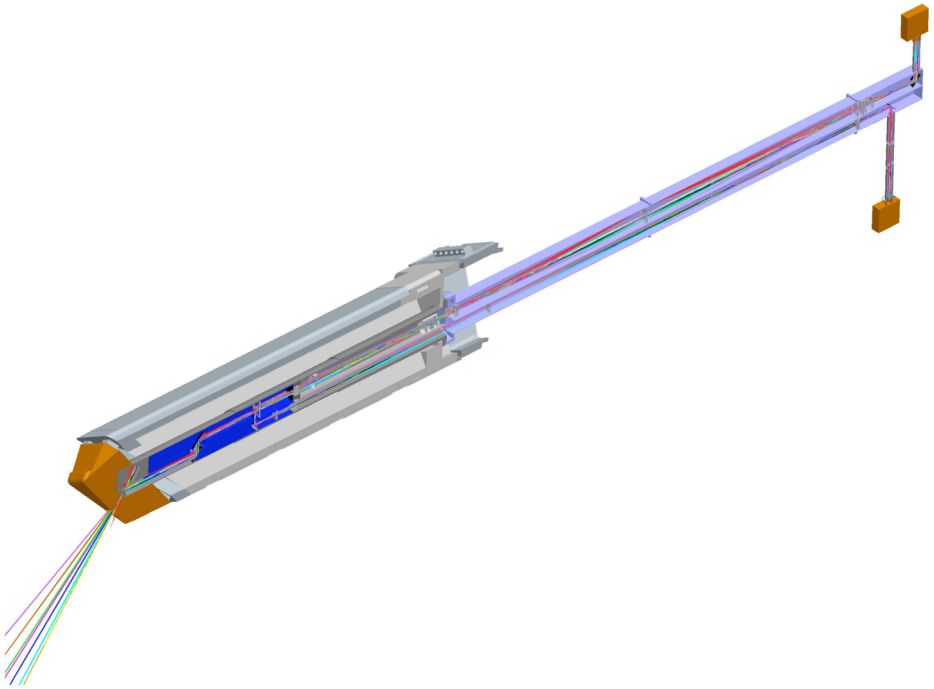

Figure 20. Cutaway view of the optical path, showing ray tracing.

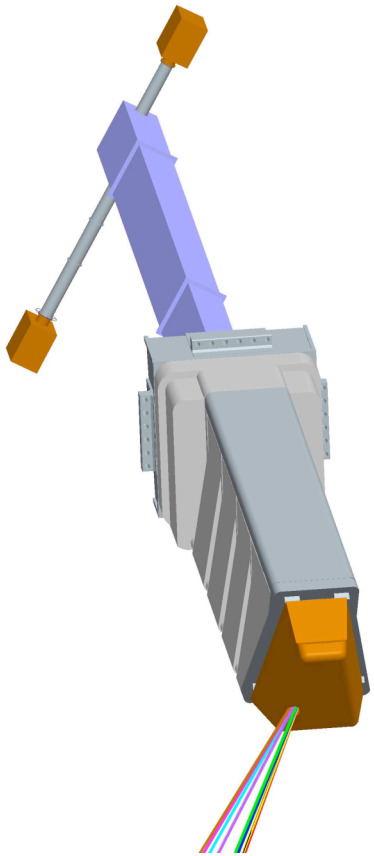

Figure 21. Port plug, optical tube, and cameras.

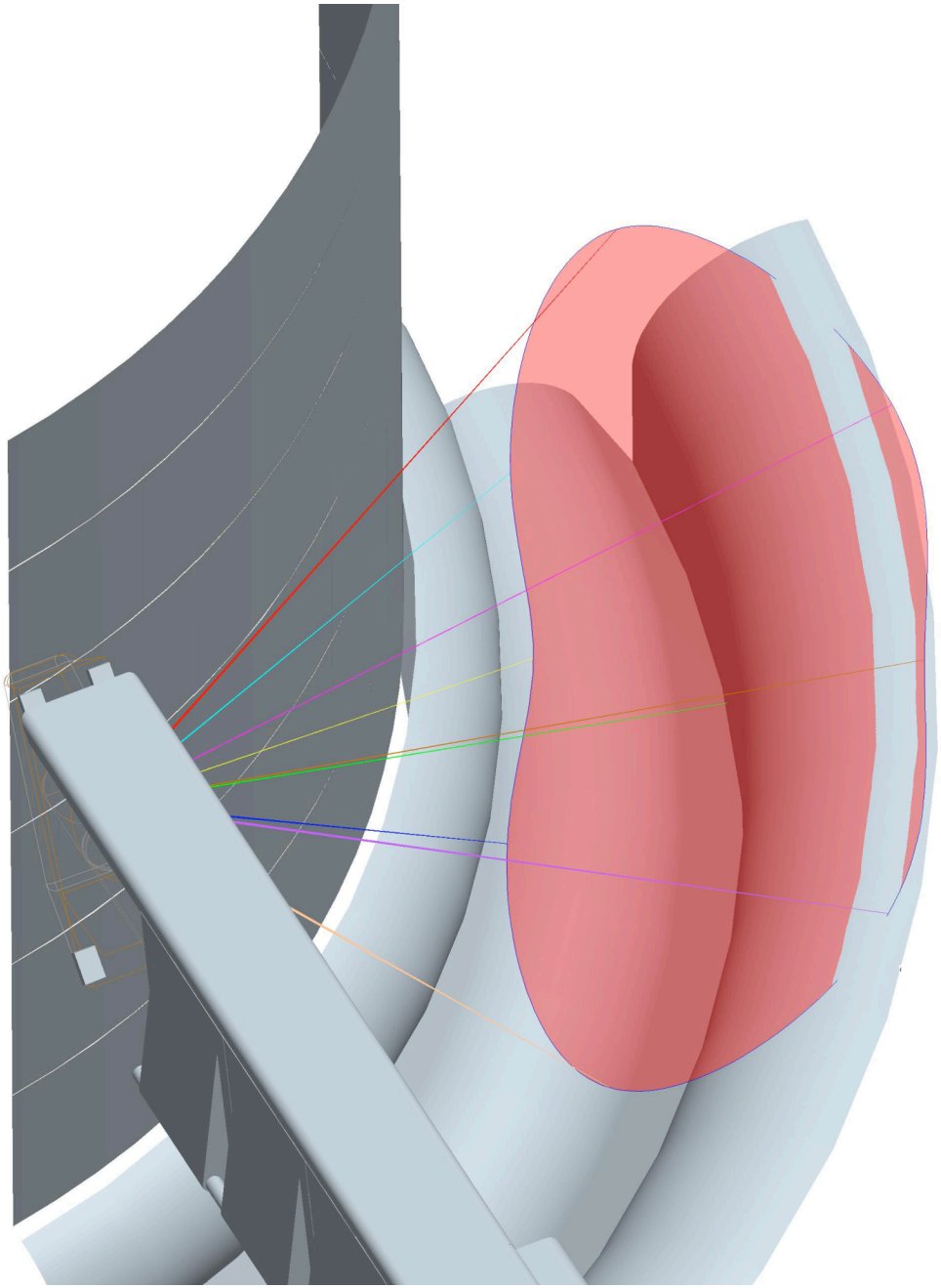

Figure 22. Field of view at the divertor.

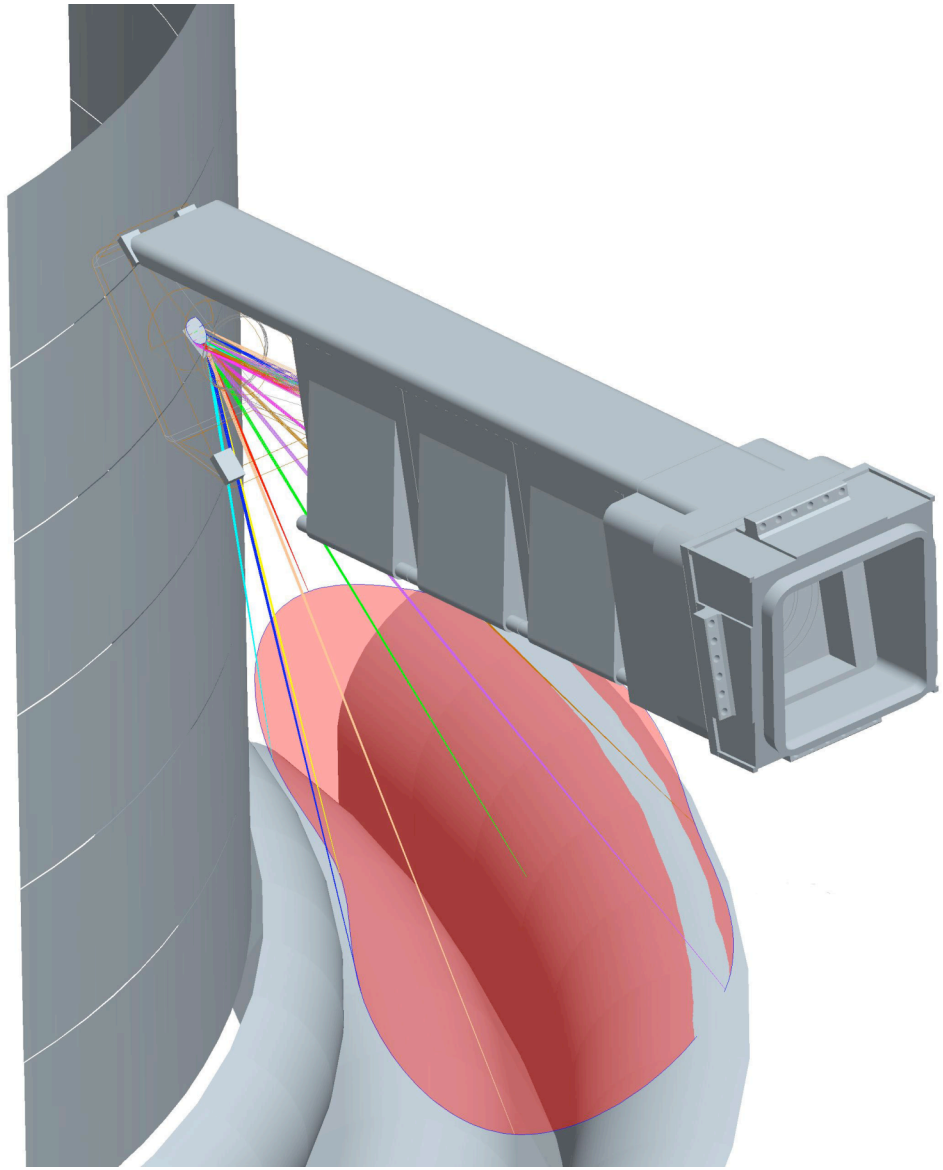

Figure 23. Another view of the port and divertor, showing the field of view.

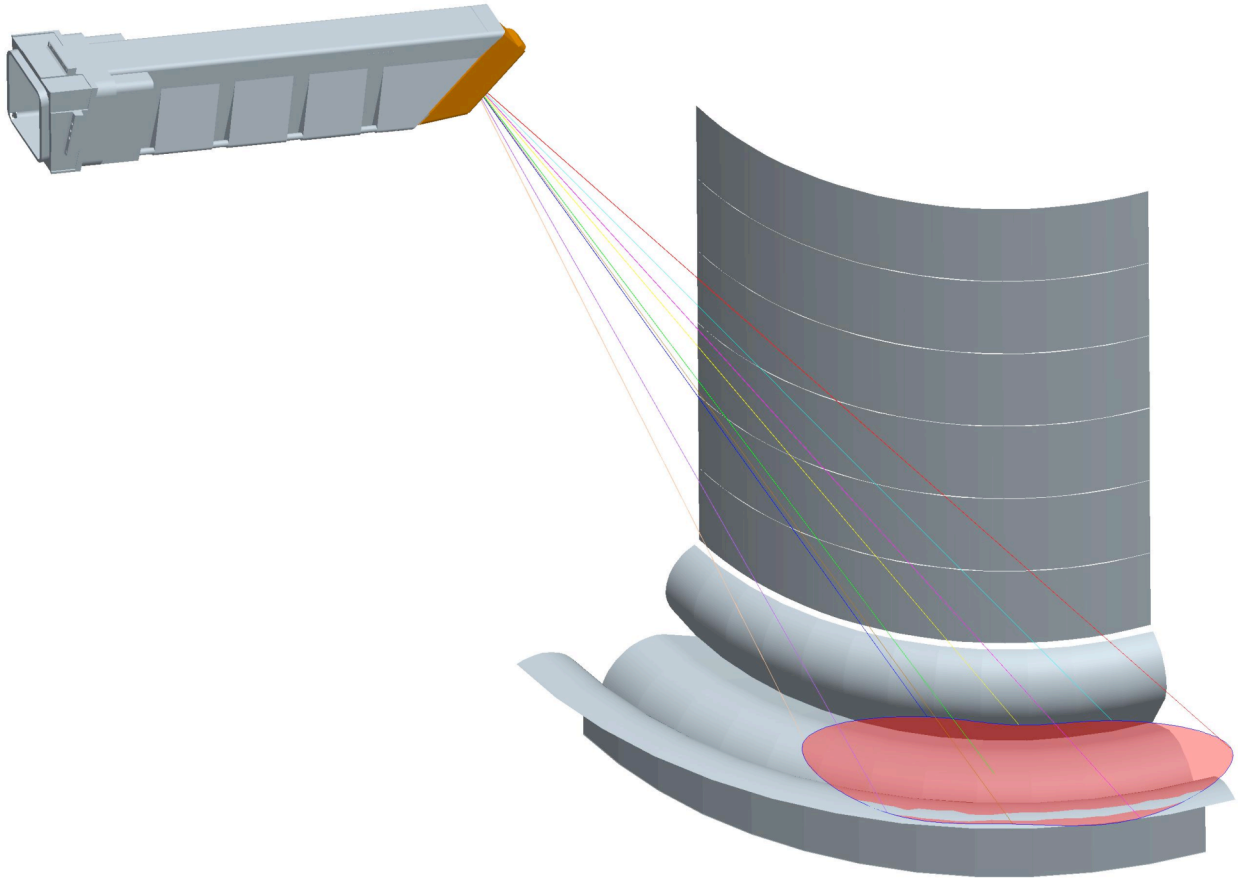

Figure 24. The camera is displaced toroidally from the viewed area.

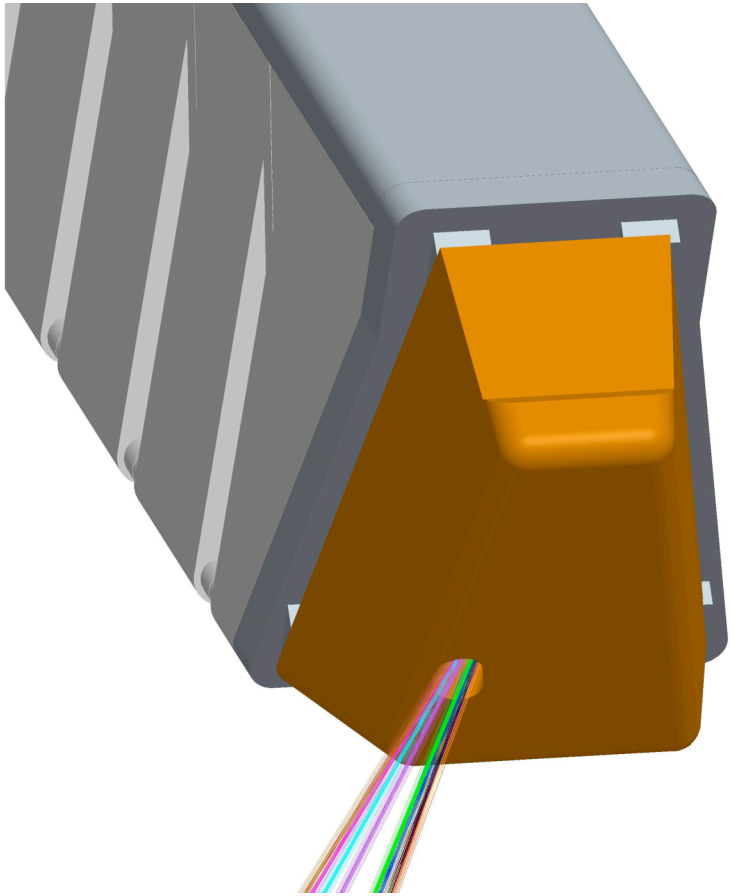

Figure 25. Viewing path through the Blanket Shield Module.

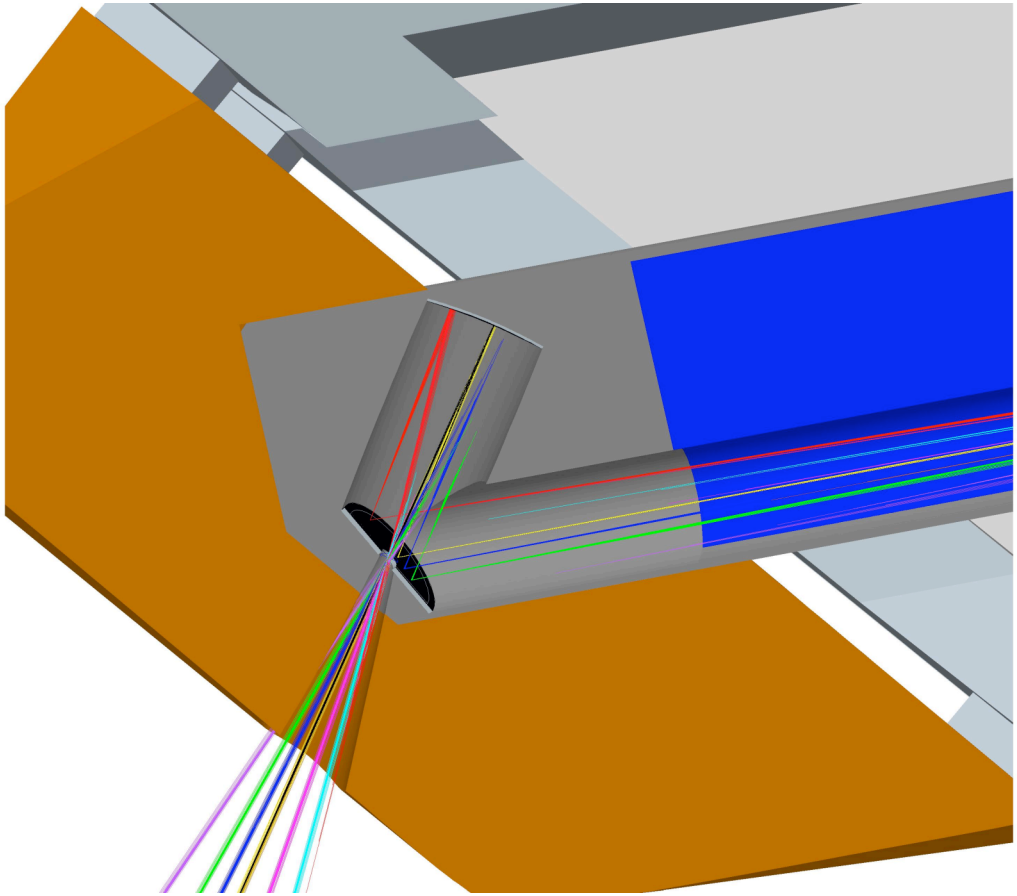

Figure 26. Side view of the optical head. The viewing aperture is located within the Blanket Shield Module for the port (solid brown area in the figure).

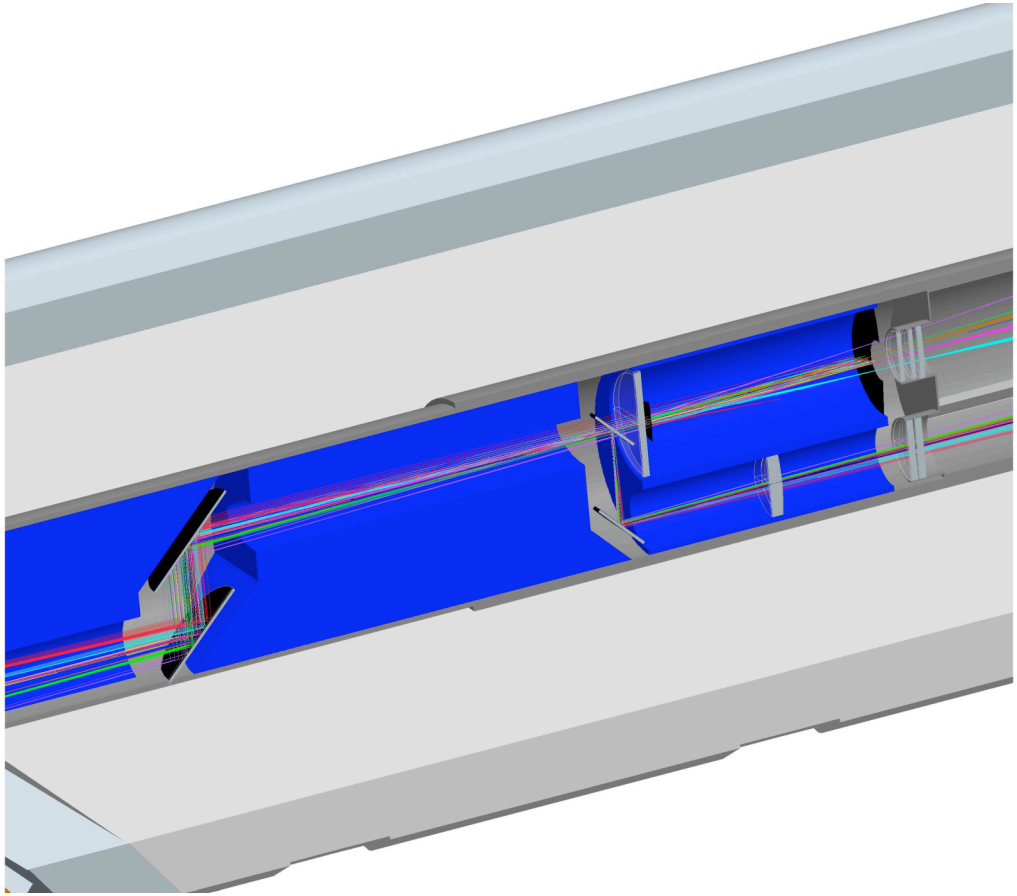

Figure 27. Side view of optics in the port plug. The blue shaded volumes represent neutron shielding, which surrounds the optics and beam path.

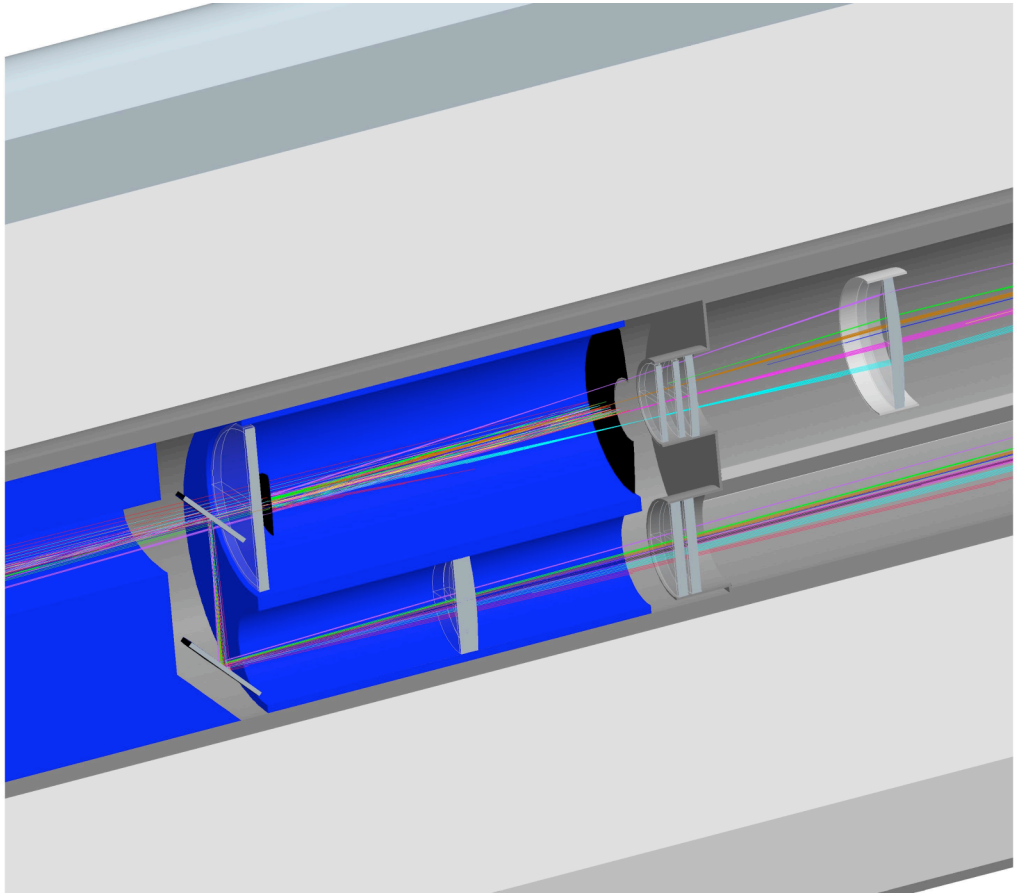

Figure 28. Expanded view of the IR Cassegrain telescope, visible light relay, and vacuum windows. The IR path has the required double vacuum windows and an adjacent corrector plate.

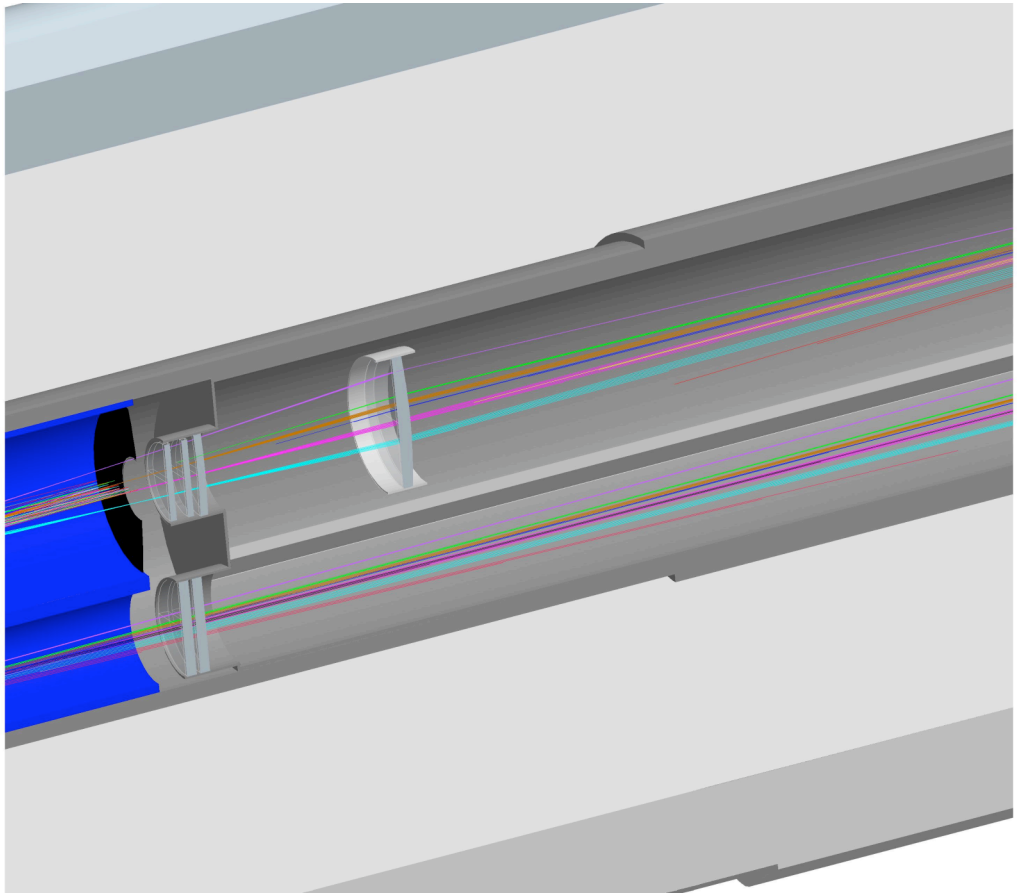

Figure 29. Expanded view of vacuum windows and an IR relay optics set.

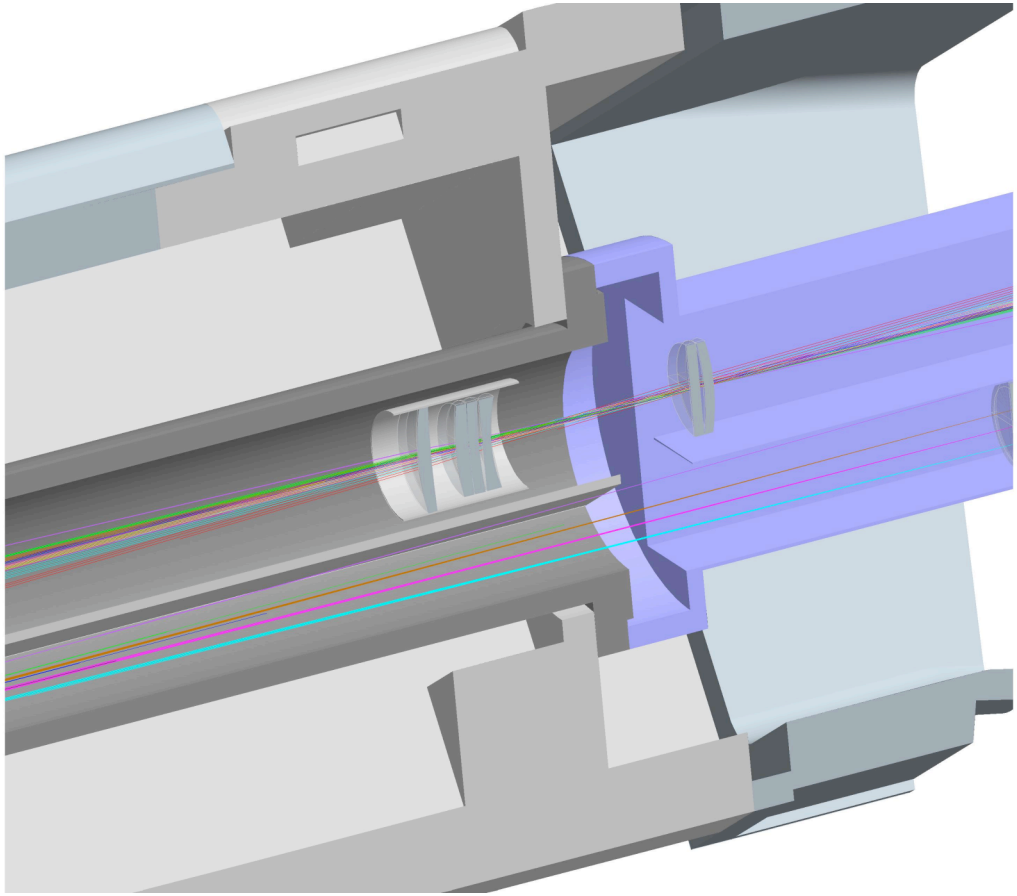

Figure 30. IR relay optics near the end of the port plug. The lower beam path is for visible light.

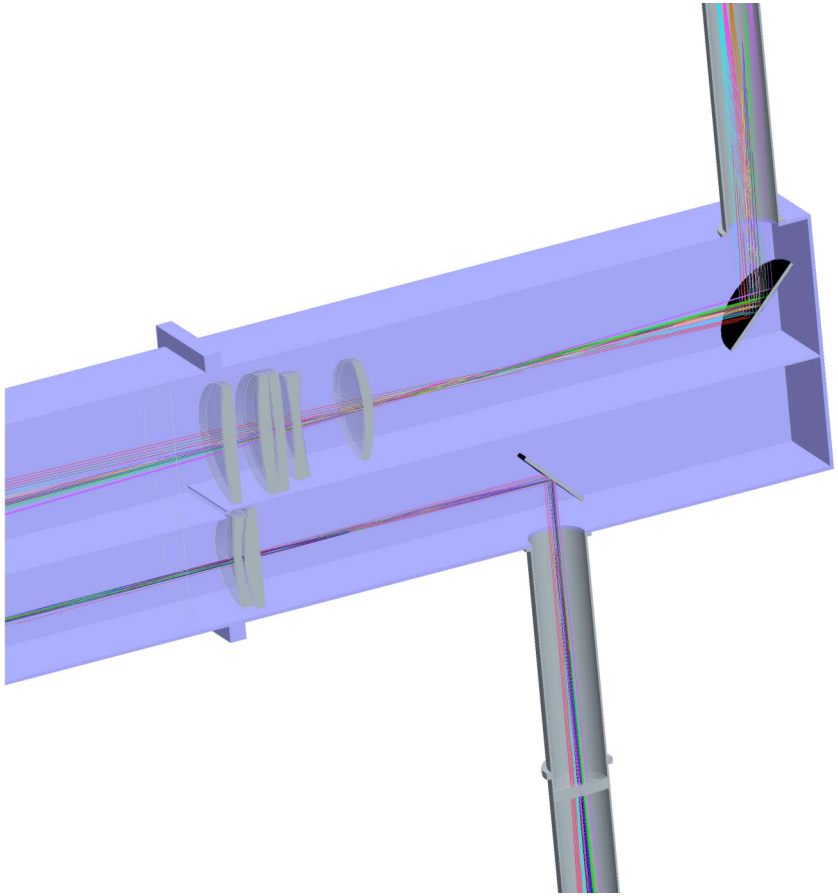

Figure 31. End section of the relay optics with turning mirrors for IR (top) and visible light (bottom).

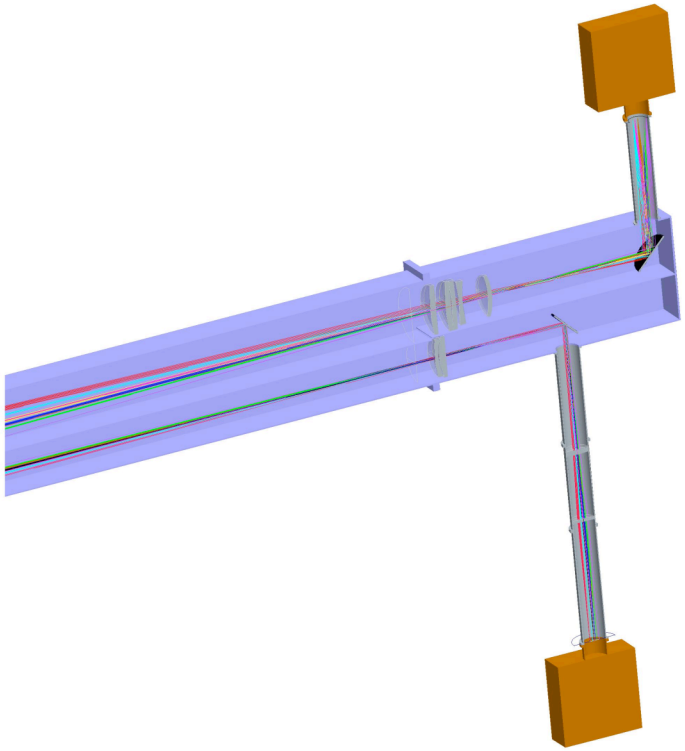

Figure 32. End section of relay optics showing IR camera (top, brown box) and visible camera (bottom, brown box). The turning mirrors allow additional shielding of the cameras from neutrons.

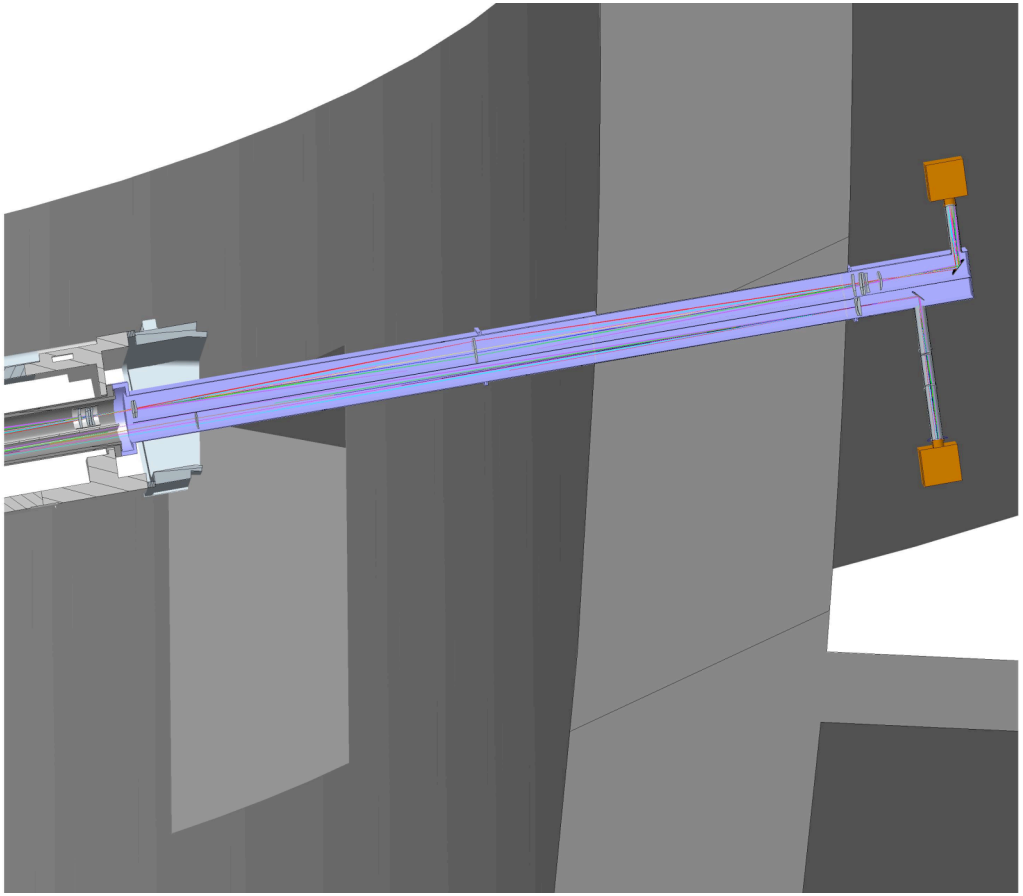

Figure 33. Outer end of port plug, optical tube across port interspace and through bioshield, with cameras.

IV. Summary

We have presented a new optical design that introduces more optics inside the port plug, and reduces the field of view from 60 toroidal degrees to 50 degrees. The IR Cassegrain telescope is now in vacuum, along with visible-light lenses replacing the visible Cassegrain. The vacuum windows are moved toward the inside on a re-entrant tube and reduced in size. The entrance aperture is increased from 10 mm to 21 mm, with a corresponding improvement is spatial resolution. The Airy disk diameter for 3.8 μm IR is now 5.1 mm at the most distant location in the view. This is still not quite as good as the ITER-specified 3 mm spatial resolution. However, 50% of the energy is captured from within a 3 mm circle diameter. Neutron shielding has been schematically added to facilitate future neutronics calculations. The entrance aperture was moved forward into the Blanket Shield Module so that cuts through adjacent modules are unneeded. The direction of view was corrected to be consistent with the fish-scale divertor design. The vacuum window diameters are now 9.4 cm clear aperture for both visible and IR. Allowing for sealing, this gives a full window diameter of 13.5 to 14 cm. A 6-inch window would be more than adequate.